

Two scenarios of spin-transfer switching and criteria for the corresponding threshold currents

Inti Sodemann^{1,2} and Ya. B. Bazaliy^{1,3,*}¹*Department of Physics and Astronomy, University of South Carolina, Columbia, South Carolina 29208, USA*²*Physics Department, University of Texas, Austin, Texas 78712, USA*³*Institute of Magnetism, National Academy of Science, Kyiv 03142, Ukraine*

(Received 28 November 2010; revised manuscript received 7 July 2011; published 23 August 2011)

It is useful to classify the spin-transfer switching events according to the scenarios of equilibrium destabilization: a local transformation or an equilibrium merging. We derive an invariant expression for the critical current of local transformation, discuss the critical current of merging, and consider the competition of the two scenarios. The critical current of saddle-point stabilization is also derived. Our results provide a intuitive picture for the behavior of spin-transfer devices, allowing one to make qualitative predictions and understand the limitations of some frequently used approximations.

DOI: [10.1103/PhysRevB.84.064422](https://doi.org/10.1103/PhysRevB.84.064422)

PACS number(s): 72.25.-b, 85.75.-d

I. INTRODUCTION

High-density electric currents induce magnetization motion and switching in nanosize metallic wires containing alternating ferromagnetic and nonmagnetic layers (Fig. 1). This phenomenon is finding important applications in computer memory and logic devices. Switching is caused by the spin-transfer torque τ_{st} ^{1,2} which depends on the magnitude and spin polarization of current, material parameters, and geometry of the device. Once the spin torque τ_{st} is found from experiment or theory, the magnetization dynamics can be obtained by solving the Landau-Lifshitz-Gilbert (LLG) equation. A simple but often sufficiently accurate approximation is the macrospin model that assumes uniform magnetization of the layer $\mathbf{M}(r,t) = M\mathbf{n}(t)$, where M is the saturation magnetization value and \mathbf{n} is a unit vector. In this case the LLG equation reads

$$\dot{\mathbf{n}} = \left[-\frac{\partial \varepsilon}{\partial \mathbf{n}} \times \mathbf{n} \right] + \tau_{st}(\mathbf{n}) + \alpha[\mathbf{n} \times \dot{\mathbf{n}}], \quad (1)$$

where $\varepsilon(\mathbf{n}) = (\gamma/M)E(\mathbf{n})$, E is the magnetic energy per unit volume, γ is the gyromagnetic ratio, and α is the Gilbert damping constant. The spin-transfer torque is proportional to electric current, $\tau_{st} \sim I$.

At $I = 0$ vector \mathbf{n} assumes an equilibrium position $\mathbf{n}_{eq}(0)$ at a minimum of magnetic energy. A nonzero current has two effects: First, the spin torque gradually shifts the equilibrium away from its original position $\mathbf{n}_{eq}(0) \rightarrow \mathbf{n}_{eq}(I)$. Second, a stable equilibrium may abruptly turn unstable at a critical current I_c . Such local loss of stability will cause a magnetic switching² to another stable state. Local destabilization is, however, not the only process leading to switching. As will be discussed below, another scenario involves a collision and disappearance of two equilibria as they shift toward each other in response to the increasing spin torque. In this paper we obtain new results for the critical current in local and merging scenarios and discuss situations where the two mechanisms compete with each other.

Various stabilization and destabilization scenarios are well understood for general dynamic systems in terms of the bifurcation theory.³ However, in the spin-transfer literature the usage of this language did not become a common practice. In part this happened because the critical current

can be found without establishing the exact scenario of the stability change. Consider, for example, a computation of the destabilization current I_c for a given stable equilibrium. The LLG equation is linearized near the point $\mathbf{n}_{eq}(I)$, resulting in a system of two coupled linear differential equations for small deviations. The stability of the equilibrium is determined by the eigenvalues $\lambda_{1,2}(I)$ of the corresponding 2×2 matrix. When the inequalities $\text{Re}[\lambda_{1,2}] < 0$ are satisfied, the equilibrium is stable. If the real part of either eigenvalue changes its sign as the current is increased, the equilibrium becomes unstable. The critical current can be determined from

$$\text{Re}[\lambda(I_c)] = 0. \quad (2)$$

Equation (2) is applicable for any destabilization scenario. But, as we show below, knowing the actual scenario one can qualitatively understand the parameters determining the critical currents and predict the qualitative behavior of the spin-transfer device above and below the current threshold.

Sections II and III of the paper discuss the local and merging scenarios, derive expressions for the critical currents, and consider examples of device operation. In Sec. IV the competition between the two scenarios is considered. There we show how our method can provide a qualitative picture of the device with several switching possibilities.

II. LOCAL CHANGE OF STABILITY

A. Motivation

In the absence of the current, the equilibrium $\mathbf{n}_{eq}(0)$ corresponds to a local minimum of the energy. It is a stable focus with two complex conjugated eigenvalues $\lambda_2 = \lambda_1^*$. Both of them have a negative real part which is a consequence of the positive damping $\alpha > 0$. (For zero damping the LLG equation describes conservative dynamics with purely imaginary values of $\lambda_{1,2}$.) To find I_c from the condition (2) one generally has to calculate two complex eigenvalues as a function of current. This calculation should, in particular, account for the displacement of the equilibrium point caused by the spin torque. The procedure is mathematically clear but does not have an obvious physical interpretation. The conventional intuition, stating that the energy minima

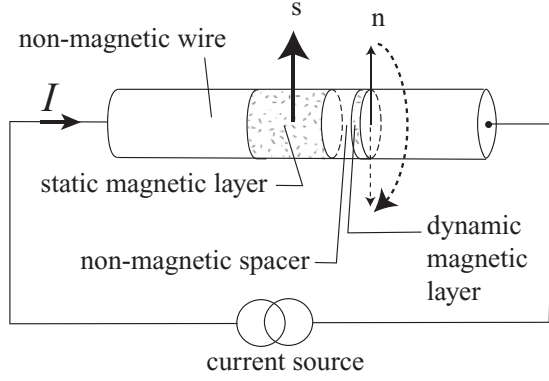


FIG. 1. Spin-transfer device with a static spin polarizer (fixed layer) and a dynamic magnet (free layer).

should be stable and the energy maxima and saddle points should be unstable, breaks down in the presence of the spin torque.

There is, however, one case where the physics of the process is well understood, namely the case of collinear geometry, where the spin polarization of the current is parallel to the equilibrium direction $\mathbf{n}_{eq}(0)$ (see, e.g., Ref. 4). Here the spin torque points opposite to the dissipation torque and directly competes with it. For the collinear geometry the effect of spin transfer is described by an additional “negative damping” $\alpha_{st} < 0$ that should be added to the original positive damping α . As soon as the total damping $\alpha_{\text{eff}} = \alpha + \alpha_{st}$ changes its sign, the equilibrium becomes unstable. The novel negative damping α_{st} introduced in the collinear case is proportional to the spin-torque magnitude, which is, in turn, proportional to the current $|\alpha_{st}| \sim |\tau_{st}| = A_{sw}I$. The coefficient A_{sw} gives a measure of the effectiveness of the current in destabilizing the equilibrium: The larger it is, the smaller the critical current will be.

The existence of a single number A_{sw} characterizing the “switching ability” of the current greatly simplifies the understanding of switching in the collinear geometry. Historically it was often implicitly assumed that the ratio $|\tau_{st}|/I$ will also play the role of switching ability for an arbitrary angle between \mathbf{n}_{eq} and spin polarization. This view, in particular, predicted that a sharp difference should exist between the destabilization of collinear and noncollinear equilibria because the spin torque is necessarily small near a collinear equilibrium [in this case $\tau_{st}(\mathbf{n}_{eq}) = 0$] but can have a finite value near a noncollinear one. The noncollinear equilibria were thus thought to have much lower critical currents. Actual calculations using the LLG linearization method, as well as experiments, did not confirm this prediction and it was argued⁴ that the critical current should generally depend not just on $|\tau_{st}|$ but also on its derivatives.

One can ask whether it is at all possible to have a single “switching ability” parameter A_{sw} characterizing the effectiveness of the current-induced destabilization in a general noncollinear geometry. Here we show that such a parameter can be indeed introduced for extremum (minimum or maximum) energy points and in some cases for energy saddle points, and find explicit expressions for it.

B. Invariant criterion, switching ability, and critical circles

The LLG equation (1) can be equivalently written as

$$(1 + \alpha^2) \dot{\mathbf{n}} = \mathbf{F}(\mathbf{n}) \equiv \boldsymbol{\tau}(\mathbf{n}) + \alpha \mathbf{n} \times \boldsymbol{\tau}(\mathbf{n}), \quad (3)$$

where $\boldsymbol{\tau} = \boldsymbol{\tau}_c + \boldsymbol{\tau}_{st}$ and $\boldsymbol{\tau}_c = -[(\partial\epsilon/\partial\mathbf{n}) \times \mathbf{n}]$ is the conservative part of the torque due to magnetic anisotropy energy and external magnetic field. Both torques $\boldsymbol{\tau}_c$ and $\boldsymbol{\tau}_{st}$ are tangent to the unit sphere.

The equilibrium magnetization orientations \mathbf{n}_{eq} satisfy $\boldsymbol{\tau}(\mathbf{n}_{eq}) = 0$. Their stability can be investigated by linearizing the equation of motion. In standard spherical coordinates (ϕ, θ) one decomposes $\mathbf{F} = F^\phi \mathbf{e}_\phi + F^\theta \mathbf{e}_\theta$ in terms of the unit vectors $\mathbf{e}_\phi, \mathbf{e}_\theta$ pointing along the coordinate lines and obtains

$$\begin{pmatrix} \delta\dot{\phi} \\ \delta\dot{\theta} \end{pmatrix} = \begin{pmatrix} \frac{1}{\sin\theta} \frac{\partial F^\phi}{\partial\phi} & \frac{1}{\sin\theta} \frac{\partial F^\phi}{\partial\theta} \\ \frac{\partial F^\theta}{\partial\phi} & \frac{\partial F^\theta}{\partial\theta} \end{pmatrix} \begin{pmatrix} \delta\phi \\ \delta\theta \end{pmatrix} = \hat{D} \begin{pmatrix} \delta\phi \\ \delta\theta \end{pmatrix}. \quad (4)$$

Stability of an equilibrium requires both eigenvalues of the “dynamic matrix” \hat{D} to have negative real parts. For a 2×2 matrix this is equivalent to the conditions (see Appendix A)

$$\text{Tr}\hat{D}(\mathbf{n}_{eq}) < 0, \quad \det\hat{D}(\mathbf{n}_{eq}) > 0. \quad (5)$$

We will call the above a “trace condition” and a “determinant condition.”

The dynamic matrix \hat{D} is not covariant with respect to the change of spherical coordinates, and its trace and determinant depend on the coordinate choice. Let us introduce a related matrix of covariant derivatives

$$\hat{D}_{\text{cov}} = \begin{pmatrix} \frac{1}{\sin\theta} \frac{\partial F^\phi}{\partial\phi} + \frac{\cos\theta}{\sin\theta} F^\theta & \frac{1}{\sin\theta} \frac{\partial F^\phi}{\partial\theta} \\ \frac{\partial F^\theta}{\partial\phi} - \cos\theta F^\phi & \frac{\partial F^\theta}{\partial\theta} \end{pmatrix}.$$

The trace of \hat{D}_{cov} is an invariant quantity equal to

$$\text{Tr}\hat{D}_{\text{cov}} = \text{div}\mathbf{F} = \frac{1}{\sin\theta} \left[\frac{\partial}{\partial\theta} (\sin\theta F^\theta) + \frac{\partial F^\phi}{\partial\phi} \right],$$

where $\text{div}\mathbf{F}$ is understood as the divergence of the vector field $\mathbf{F}(\mathbf{n})$ on the surface of a unit sphere. Crucially, at equilibrium points the original and the invariant dynamic matrices are equal, $\hat{D} = \hat{D}_{\text{cov}}$, and we can use $\text{Tr}\hat{D}_{\text{cov}} < 0$ and $\det\hat{D}_{\text{cov}} > 0$ instead of (5). In particular, an invariant condition $\text{div}\mathbf{F} < 0$ replaces the trace condition.

The trace condition describes the local destabilization or stabilization of the equilibria corresponding to the energy extrema (minima and maxima). In those cases $\det\hat{D} > 0$, and the stability change is due to the sign change of $\text{Tr}\hat{D} = \text{div}\mathbf{F}$.

Using the relation between \mathbf{F} and $\boldsymbol{\tau}$ and notation $\text{div}\mathbf{F} = \nabla \cdot \mathbf{F}$, we find

$$\nabla \cdot \mathbf{F} = \nabla \cdot \boldsymbol{\tau} - \alpha [\nabla \times \boldsymbol{\tau}] \cdot \mathbf{n}, \quad (6)$$

where $[\nabla \times \boldsymbol{\tau}] \cdot \mathbf{n} = -[\partial\tau_\theta/\partial\phi - \partial(\sin\theta\tau_\phi)/\partial\theta]/\sin\theta$ is the curl of the field $\boldsymbol{\tau}$ on the surface of the sphere.

The general expression for the spin-torque created by a polarizer pointing along the unit vector \mathbf{s} reads⁵

$$\boldsymbol{\tau}_{st}(\mathbf{n}, I) = \omega_I g(\mathbf{n} \cdot \mathbf{s}) [\mathbf{n} \times (\mathbf{s} \times \mathbf{n})] \equiv \omega_I \mathbf{f}_{st}(\mathbf{n}). \quad (7)$$

Here $\omega_I = (\gamma/M)(\hbar I/2eV)$ is the rescaled current, where V is the magnetic layer volume, e is the electron charge, and

$g(\mathbf{n} \cdot \mathbf{s})$ is the efficiency factor.⁶ In the last form of spin torque we have explicitly separated the overall proportionality to the current from the angular dependence $\mathbf{f}_{st}(\mathbf{n})$. Importantly, the conservative torque is divergence free,

$$\nabla \cdot \boldsymbol{\tau}_c = 0,$$

and the spin-transfer torque is curl free,

$$[\nabla \times \boldsymbol{\tau}_{st}] \cdot \mathbf{n} = 0.$$

Using these properties we get

$$\nabla \cdot \mathbf{F} = \nabla \cdot \boldsymbol{\tau}_{st} - \alpha \nabla \times \boldsymbol{\tau}_c = \omega_I \nabla \cdot \mathbf{f}_{st} - \alpha \nabla^2 \varepsilon. \quad (8)$$

By changing the current, one can control the sign and magnitude of the first term and produce the sign change of the whole expression. We see that the switching ability $A_{sw} = \nabla \cdot \mathbf{f}_{st}$ exists and is determined by the divergence of the quantity $\mathbf{f}_{st}(\mathbf{n})$ characterizing the angular dependence of the spin torque.

Additionally, equation (8) shows that the condition $\text{div} \mathbf{F} = 0$ can be viewed as a limiting case of the condition for the existence of a precession state (PS). A precession cycle is characterized by the integral condition $\oint (\boldsymbol{\tau}_{st} \cdot \mathbf{e}_\perp) dl = \alpha \oint (\nabla \varepsilon \cdot \mathbf{e}_\perp) dl$, where \mathbf{e}_\perp is a unit vector perpendicular to the cycle trajectory and tangent to the sphere, and the integrals are taken along the cycle.⁷⁻⁹ This integral condition reflects the balance of incoming and dissipated energy. As the size of the cycle tends to zero, Eq. (8) is recovered from the integral condition. In terms of the bifurcation theory³ local destabilization of the minimum points is the *Hopf bifurcation* which normally produces a small stable precession cycle around the destabilized equilibrium.

Consider now the experimentally relevant case of small Gilbert damping, $\alpha \ll 1$. Expression (8) shows that the critical current satisfies $I_c \propto \alpha$ and hence will be also small. Therefore at $I = I_c$ the equilibrium point $\mathbf{n}_{eq}(I_c) = \mathbf{n}_{eq}(0) + \Delta \mathbf{n}$ will be close to $\mathbf{n}_{eq}(0)$ with $\Delta \mathbf{n} \propto I_c \propto \alpha$. Expanding (8) up to linear terms in α we get an approximate stability condition

$$\omega_I \nabla \cdot \mathbf{f}_{st}|_{\mathbf{n}_{eq}(0)} \leq \alpha \nabla^2 \varepsilon|_{\mathbf{n}_{eq}(0)} \quad (9)$$

with equality achieved at the critical current.⁵ Importantly, all quantities in (9) are evaluated at the unperturbed equilibrium point $\mathbf{n}_{eq}(0)$. In comparison, using conditions (5) one needs^{6,12} to perform an explicit calculation of $\mathbf{n}_{eq}(I_c)$ even in the case of the first-order expansion in α . This situation is discussed in more detail in Appendix B.

According to Eq. (9) the critical current is given by

$$\omega_{Ic} = \alpha \frac{\nabla^2 \varepsilon|_{\mathbf{n}_{eq}(0)}}{A_{sw}}. \quad (10)$$

In this formula the influences of the magnetic energy and of the spin torque on the critical current are completely separated. The former determines the equilibrium point $\mathbf{n}_{eq}(0)$ and the value of the numerator, and the latter is responsible for the switching ability standing in the denominator. For example, if one would rotate the polarizer \mathbf{s} keeping the energy ε constant, the critical current would change according to the dependence of A_{sw} on the angle between \mathbf{s} and $\mathbf{n}_{eq}(0)$.

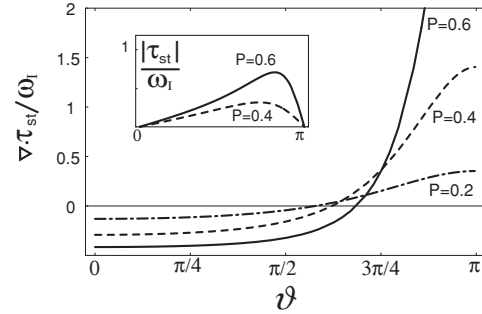


FIG. 2. Angular dependence of the spin-torque divergence. Efficiency factor is taken in the Slonczewski form. Inset: Absolute value of spin torque. Curves for different spin polarizations P are shown.

We now derive a useful expression for the switching ability $A_{sw} = \nabla \cdot \mathbf{f}_{st}$. For $\boldsymbol{\tau}_{st}$ given by Eq. (7) one gets

$$\nabla \cdot \mathbf{f}_{st} = -\frac{1}{\sin \vartheta} \frac{d}{d\vartheta} [g(\cos \vartheta) \sin^2 \vartheta], \quad (11)$$

where ϑ is the angle between \mathbf{s} and \mathbf{n} . Representative graphs of $\nabla \cdot \mathbf{f}_{st}(\vartheta)$ are shown in Fig. 2 for the Slonczewski form² of $g(\vartheta)$. We observe the following:

(a) The angular dependence of the divergence $\nabla \cdot \boldsymbol{\tau}_{st}(\vartheta)$ differs substantially from that of $|\boldsymbol{\tau}_{st}|(\vartheta)$. In particular, the divergence is not necessarily small in the collinear configurations $\vartheta = 0, \pi$ and the destabilization of noncollinear equilibria may actually require larger currents than those needed for the collinear cases.

(b) The switching ability $A_{sw} = \nabla \cdot \mathbf{f}_{st}$ vanishes at a critical angle ϑ_* [Fig. 2]. Equation (10) predicts infinite critical current for the equilibrium points lying on the “critical circle” (CC) defined by $\vartheta(\phi, \theta) = \vartheta_*$ [more precisely, the approximation (9) breaks down at CC and I_c is just large]. The critical circle divides the unit sphere into two parts. Spin-transfer torque destabilizes the energy extrema in one of them (which one depends on the current direction), while in the other it makes them more stable.

(c) The signs of I_c are opposite for equilibria located on different sides of a CC. This circumstance is especially relevant when one considers different models of $g(\vartheta)$. For example in the Slonczewski case ϑ_* depends on the spin polarization P and varies from $\vartheta_*(P=0) \gtrsim \pi/2$ to $\vartheta_*(P=1) = \pi$. In contrast, for a popular approximation $g = \text{const}$, one has $\vartheta_* = \pi/2$ independently of P . The difference between the two models becomes crucial for an equilibrium located between the respective CCs: A given current would have a stabilizing effect in one model, and destabilizing in another.

(d) In the collinear geometry $\vartheta = 0, \pi$ and the spin-torque divergence (11) is reduced to $2g(0)$ and $2g(\pi)$, respectively. Thus in these cases A_{sw} is indeed proportional to the spin-torque magnitude, in accord with the physical picture presented in Sec. II A.

C. Examples

Let us now show how the notions of switching ability and critical circles allow one to understand qualitatively the behavior of various devices. Note that expression (10)

is ultimately based on the smallness of the equilibrium displacement for $\alpha \ll 1$ and $\omega_I \lesssim \omega_{Ic}$. This property allows one to classify each equilibrium by its position $\mathbf{n}_{eq}(0)$ at zero current. In this spirit we will refer to the finite current equilibria $\mathbf{n}_{eq}(I)$ as energy minima and maxima. We will consider typical nanopillars¹⁰ with an (x, y) easy plane and an easy axis $\mathbf{v} \parallel \hat{x}$, so that

$$\varepsilon = \frac{1}{2}\omega_p(\mathbf{n}\hat{z})^2 - \frac{1}{2}\omega_a(\mathbf{n}\mathbf{v})^2 - \gamma(\mathbf{H} \cdot \mathbf{n}),$$

where ω_p and $\omega_a < \omega_p$ are the easy plane and easy axis anisotropy constants. Nanopillar devices differ in the directions of applied field \mathbf{H} and spin polarizer \mathbf{s} .

1. Example 1

First, let the external magnetic field $\mathbf{H} \parallel \hat{y}$ be applied in the easy plane, perpendicular to \mathbf{v} , and the polarizer be directed along the easy axis, $\mathbf{s} \parallel \mathbf{v}$ (Fig. 3). In the absence of applied field the energy minima M_1 and M_2 are located at $\pm\mathbf{v}$. As the field is turned on, the minima move along the equator toward the saddle point L , and finally merge with it when the field reaches the easy axis anisotropy value $H_A = \omega_a/\gamma$. For this case the spin-transfer switching diagrams in the plane of parameters (H, I) were calculated in Refs. 11 and 12. The diagrams for a generic efficiency function $g(\vartheta)$ [Fig. 3(a)] and for the special case of $g = \text{const}$ [Fig. 3(b)] are found to be qualitatively different, with the former diagram displaying the “anomalous” region [Fig. 3(a)] where both critical currents are negative. In our approach the occurrence of an “anomaly” is naturally explained by the fact that the minimum point $M_1(H)$ crosses the critical circle at $H = H_*$. After the crossing both equilibria are found on the same side of CC and are destabilized by the current of the same direction. For $g = \text{const}$ the critical angle is $\vartheta_* = \pi/2$ and the minima never cross the critical circle; hence the anomalous region is absent. The

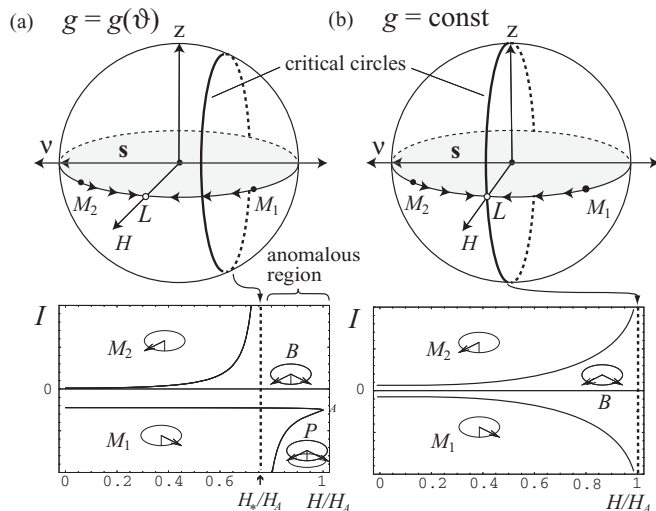


FIG. 3. Critical circles and the “anomalous” stabilization region. Upper panels: Collinear device with $\mathbf{s} \parallel \mathbf{v} \parallel \hat{x}$ and $\mathbf{H} \parallel \hat{y}$. The energy minimum points M_1 and M_2 move with increasing H as shown by the arrows. Critical circles shown for (a) generic $g(\vartheta)$ and (b) $g = \text{const}$. Lower panels: Switching diagrams. In the regions M_1 and M_2 one equilibrium is stable, in B both are stable, and in P both are unstable.

$\tau_{st}(\vartheta)$ dependence produced by the $g = \text{const}$ approximation is qualitatively similar to the actual one. Nevertheless, it does not lead to the correct qualitative picture of switching when the equilibria of interest are close to the actual critical circle.

2. Example 2

The previous example discussed spin-transfer destabilization of an energy minimum. Equation (9) can also describe the opposite process of an energy-maximum stabilization. At an energy-maximum point the Laplacian satisfies $\nabla^2\varepsilon < 0$, so the term $\omega_I \nabla \cdot \mathbf{f}_{st}$ has to become sufficiently negative to stabilize the equilibrium. The critical value of ω_I is again determined from Eq. (10). Stabilization of the energy maximum was first discussed in Ref. 13 for a simple anisotropy. In the nanopillar case such a stabilization was studied in Ref. 6 in the case of external field and spin polarization directed along the easy axis, $\mathbf{H} \parallel \mathbf{v}$, $\mathbf{s} \parallel \mathbf{v}$. It was found that the stabilization current diverges and changes its sign at a particular field H_* . The reason for this peculiar dependence was not understood at the time. With the present insight the picture becomes clear. The energy-maximum point is shifted by the changing magnetic field and crosses the critical circle at $H = H_*$. This crossing naturally explains the behavior of the corresponding critical current.⁶

3. Example 3

Sensitivity to the $g(\theta)$ angular dependence turns out to be of crucial importance for the interpretation of the “spin-flip transistor” precession experiment.¹⁴ The spin-flip transistor is a nanopillar with $\mathbf{s} \parallel \hat{y}$. Calculations^{19,20} performed with the assumption $g = \text{const}$ found that in this configuration the precession state is forbidden at zero magnetic field, but can exist in an external field $\mathbf{H} \parallel \hat{y}$ if it is directed antiparallel to \mathbf{s} . At the same time the precession state was experimentally observed at $H = 0$.¹⁴ Based on the theory of Refs. 19 and 20 this result was interpreted as an indication that an additional “fieldlike” term had to be introduced in Eq. (7).

Within the framework of our analysis, the absence of PS states at zero field is due to the fact that at $g = \text{const}$ and $H = 0$ the energy minima $M_{1,2}$ are located on the critical circle [Fig. 4(a)] and cannot be destabilized. The antiparallel field is required to shift the minimum points away from CC. However, for general $g(\vartheta)$, the minimum points are away from CC even at $H = 0$ [Fig. 4(b)]. They can be locally destabilized,

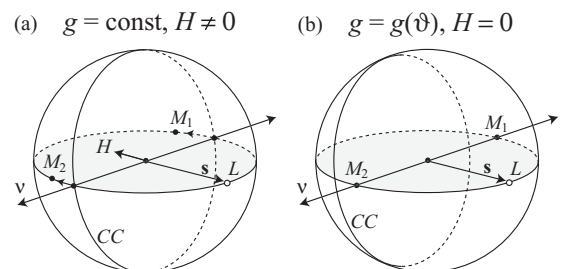


FIG. 4. Spin-flip transistor geometry. (a) For $g = \text{const}$ local destabilization of the energy minima requires external field H to shift $M_{1,2}$ away from the critical circle (marked CC). (b) For $g = g(\vartheta)$ the minima are away from CC even at $H = 0$.

producing PS states by Hopf bifurcation without any fieldlike terms.¹⁸ The lesson of this example is that the $H = 0$ results of Refs. 19 and 20 are sensitive to the angular dependence $g(\vartheta)$ in a manner that would be hard to foresee without the notion of a critical circle.

4. Example 4

To further demonstrate the power of the analysis based on Eqs. (9) and (11), consider the experiment¹⁵ performed on a nanopillar device with an unusual “wavy” $\tau_{st}(\vartheta)$ dependence.^{16,17} As Fig. 5(a) shows, in this case there are two critical circles, CC_1 and CC_2 , defined by the angles $\vartheta_{*1,2}$. At zero external field the energy minima $M_{1,2}$ fall into the regions of the same sign of $\nabla \cdot \tau_{st}$ and can be destabilized simultaneously, producing a precession cycle.¹⁵ With increasing current, the cycle gradually approaches the energy-maximum point X . Eventually spin transfer stabilizes that point⁶ by closing the contour on it.¹⁵

Here the notion of critical circles suggests an experiment capable of providing additional evidence for the “wavy” $\tau_{st}(\vartheta)$ dependence. If an $\mathbf{H} \parallel \hat{y}$ field is applied to the nanopillar [Fig. 5(b)], the energy minima $M_{1,2}$ are shifted toward the saddle point L . Since ϑ_{*1} and ϑ_{*2} are not necessarily symmetric with respect to $\pi/2$, there will be an interval of fields where M_1 has already crossed CC_1 and moved into the middle region, while M_2 remains in the left region. In this interval $\nabla \cdot \tau_{st}$ has opposite signs for $M_{1,2}$ and normal switching between M_1 and M_2 will be possible. Further increase of H will put both minimum points into the middle region, where they will be again destabilized by the same current direction. However, now the same current direction will also destabilize X , so the evolution of the PS state will be different from the $H = 0$ case.¹⁸

III. EQUILIBRIUM MERGING

Let us now turn to the question of saddle-point stabilization. In the absence of current these points are unstable with $\det \hat{D}_{I=0} < 0$, so their stabilization requires a change of sign of $\det \hat{D}$.

An example of saddle-point stabilization is provided by a spin-flip transistor in zero field where the spin torque attracts \mathbf{n} to the saddle point and eventually stabilizes L .^{19,20} Notably, this stabilization is accompanied by a simultaneous discontinuous change in the nature of two other equilibria: The

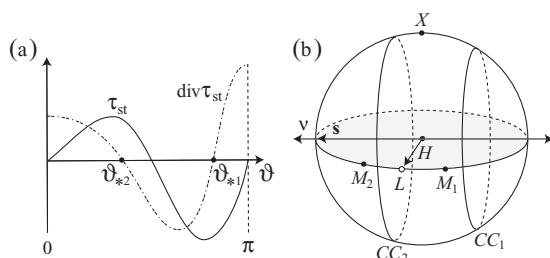


FIG. 5. (a) “Wavy” $\tau_{st}(\vartheta)$ dependence (Ref. 15) (solid line) and corresponding $\nabla \cdot \tau_{st}$ (dashed line). (b) Critical circles $CC_{1,2}$ and positions of minimum points $M_{1,2}$ at an intermediate value of the field H . The energy-maximum point is X .

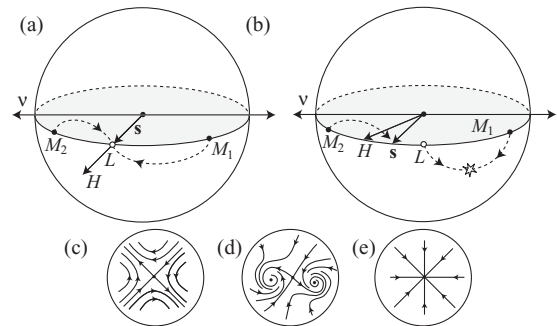


FIG. 6. (a) Spin-flip transistor: $\mathbf{s} \perp \hat{z}$, $\mathbf{s} \perp \mathbf{v}$, $\mathbf{H} \parallel \mathbf{s}$. The dashed lines show how the positions of the equilibria M_1 and M_2 change with increasing current and merge with the saddle L . (b) General in-plane directions of \mathbf{s} and \mathbf{H} . The saddle merges with one of the minima, while the other one asymptotically approaches \mathbf{s} . (c)–(e) Transformation of the field \mathbf{F} during the merging of a saddle with two foci in case (a).

minimum points $M_{1,2}$ lose their stability at the same critical current that makes L stable.¹⁹

The spin-flip transistor device at zero field has high symmetry. To get more intuition about the stabilization of saddles we first study what happens when the symmetry is reduced by an application of the magnetic field parallel to the spin polarization vector, $\mathbf{H} \parallel \mathbf{s} \parallel \hat{y}$. If the field is directed parallel to \mathbf{s} (note the difference with the antiparallel case discussed in Sec. II C, example 3), the current leads to a significant deviation of the minima $M_{1,2}$ from their initial positions [Fig. 6(a)]. The minimum points $M_{1,2}$ approach L and merge with it at the critical current, forming a stable center. The saddle-point stabilization still happens through a process involving several equilibrium points.

We start by explaining why those simultaneous transformations are not a coincidence. In the examples above the saddle point is stabilized by conversion into a stable center. However, as topological defects of the vector field \mathbf{F} , saddles and centers differ in the winding number²¹ which is a topological characteristic equal to $n = -1$ for a saddle and $n = 1$ for a center or focus. Since the total winding number is conserved according to the Poincaré index theorem, a saddle point cannot be transformed into a center locally. The saddle-to-center transformation has to either proceed via merging with other defects, or be accompanied by a simultaneous change of nature of the far-away equilibria. For example, Figs. 6(c)–6(e) show an allowed merger with two focus points, each of which has $n = 1$.

An even better insight comes from considering a generic case of \mathbf{H} and \mathbf{s} pointing in the arbitrary in-plane directions [Fig. 6(b)]. Here the saddle point L merges with one of the minima which leads to the disappearance of both equilibria. In the meantime the other minimum approaches \mathbf{s} . Merging of a saddle point and focus point ($n = 1$) is allowed by the winding-number conservation. In fact, the bifurcation theory³ shows that it is the most general case called a *saddle-node bifurcation*. As a result, the saddle point is normally not stabilized but rather destroyed in a collision with an energy-extremum point.

Note that another equilibrium destroyed in such a collision can be a stable one. In this case its disappearance will lead

to a switching event. A saddle-node bifurcation constitutes a separate switching mechanism, complementary to the local destabilization discussed in Sec. II. Here the critical current can in principle be determined by applying the condition $\det \hat{D} = 0$. However, as we have seen in the spin-flip transistor example, in this case the deviation of $\mathbf{n}_{eq}(I)$ from $\mathbf{n}_{eq}(0)$ is large. Thus one first has to calculate the actual position $\mathbf{n}_{eq}(I)$ and then find the determinant $\det \hat{D}(\mathbf{n}_{eq}(I))$. As a result, it is more practical to detect the switching moment by searching for the equilibrium collision event, without even applying the linear-stability analysis.

Returning to the stabilization of a saddle point, we see that it happens only in special circumstances, for example in an important special case when \mathbf{s} is pointing exactly into the saddle L . In such a geometry L remains an equilibrium for an arbitrarily large current and thus cannot disappear in a saddle-node bifurcation. This restriction produces a *transcritical bifurcation*³ where the energy extremum and the saddle exchange their nature in a collision. The bifurcation diagram [Fig. 7(a)] gives the positions of the colliding equilibria as a function of applied current. It is seen how the previously unstable saddle point becomes a stable center (or focus) above the critical current value.

Sometimes, e.g., in the case of a spin-flip transistor with magnetic field $\mathbf{H} \parallel \mathbf{s}$ [Fig. 6(a)], a more rare *fork bifurcation* is produced due to additional symmetries. A very rare nonlocal bifurcation exhibited by the spin-flip transistor at $\mathbf{H} = 0$ can only occur in devices of exceptionally high symmetry.

In the case of perfect transcritical bifurcation with \mathbf{s} pointing into the saddle point a simple formula can be derived for a critical current from the condition $\det \hat{D}(I_c) = 0$. First, using expression (3) for \mathbf{F} one can show that

$$\det \hat{D} = (1 + \alpha^2) \det \hat{D}|_{\alpha=0}. \quad (12)$$

The value of the determinant at $\alpha = 0$ includes, of course, both the conservative \hat{D}_c and the spin transfer \hat{D}_{st} contributions to the dynamic matrix. The critical current condition obtains the form

$$\det(\hat{D}_c|_{\alpha=0} + \hat{D}_{st}|_{\alpha=0}) = 0. \quad (13)$$

In the present case of $\mathbf{s} = \mathbf{n}_{eq}$ the derivation is more transparent if one uses special coordinates instead of employing the general expressions (4). Pointing axis \hat{z} of the polar angle system along \mathbf{s} we naturally introduce coordinates $x = \sin \theta \cos \phi$ and $y = \sin \theta \sin \phi$ with the equilibrium point at $(x, y) = (0, 0)$.

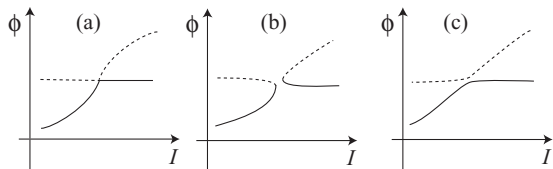


FIG. 7. Transcritical bifurcation diagram shows the positions of the two colliding equilibria as a function of current [only one angle $\phi(I)$ is shown for clarity]. Solid lines, stable equilibrium; dashed lines, unstable equilibrium. (a) Perfect bifurcation with \mathbf{s} pointing exactly into the saddle point. (b), (c) Imperfect bifurcations realized for \mathbf{s} pointing close to the saddle point.

Using the second-order expansion of the energy in small displacements

$$\varepsilon = \varepsilon(0) + \frac{1}{2}\varepsilon_{xx}x^2 + \varepsilon_{xy}xy + \frac{1}{2}\varepsilon_{yy}y^2,$$

we find

$$\hat{D}_c|_{\alpha=0} = \begin{vmatrix} -\varepsilon_{xy} & -\varepsilon_{yy} \\ \varepsilon_{xx} & \varepsilon_{xy} \end{vmatrix}.$$

For the spin-transfer contribution one gets

$$\hat{D}_{st}|_{\alpha=0} = -\omega_I \begin{vmatrix} g(0) & 0 \\ 0 & g(0) \end{vmatrix}.$$

Using these matrices in the condition (13) we find the critical current of the saddle-point stabilization to be

$$\omega_I = \frac{\sqrt{-\det \hat{D}|_{I=0, \alpha=0}}}{g(0)}. \quad (14)$$

This result can be alternatively understood as follows. The conservative torque alone creates a saddle point with eigenvalues $\lambda_1 > 0$ and $\lambda_2 < 0$. It repels \mathbf{n} from the equilibrium along the λ_1 eigenvector and attracts it along the λ_2 eigenvector. The spin-transfer torque alone creates a stable center with two equal eigenvalues $\lambda_{1,2} = -\omega_I g(0) < 0$. It equally attracts \mathbf{n} to the equilibrium along all directions. When the two are added, the equilibrium will be stable if the spin torque exceeds the conservative torque along the most repulsive direction, i.e., along the λ_1 eigenvector. Thus the condition of stabilization reads $\omega_I g(0) = \lambda_1$. The conservative torque is not arbitrary, but derived from a potential ε . As a result, the eigenvalues of \hat{D}_c satisfy $\lambda_1 = -\lambda_2$. Now one can express $\lambda_1 = \sqrt{-\det \hat{D}_c} = \sqrt{-\det \hat{D}|_{I=0, \alpha=0}}$ and recover formula (14).

For a small misalignment of \mathbf{s} and L an abrupt saddle-center transformation is replaced by a crossover in a small interval of currents. This is guaranteed by the fact that at low current the saddle point has to remain near \mathbf{s} and at large current a stable equilibrium near \mathbf{s} is inevitably produced by the increasing attraction of \mathbf{n} to \mathbf{s} . The crossover can happen in two ways [Figs. 7(b) and 7(c)]. Case (b) is a generic destruction and creation of the saddle-center pair. Case (c) is formally not a bifurcation, but looks like one for all practical purposes if the misalignment is small. Formula (14) remains a good estimate for the crossover current, although to get the full picture of the imperfect bifurcation one has to follow the positions of both equilibria in the region of their anomalous approach to each other.

IV. COMPETITION BETWEEN THE TWO DESTABILIZATION SCENARIOS

As discussed in Sec. III, local destabilization of an energy minimum and merging with a saddle point are the two alternative switching mechanisms. We know from Sec. II that the critical current of local destabilization is proportional to a small parameter α . The critical current of merging, determined from $\det \hat{D}(I_c) = 0$, is independent of α due to the relationship (12). Physically, local destabilization results from a competition of the negative damping brought by the spin torque with the small positive Gilbert damping. In contrast, equilibrium merging results from the competition between

the spin torque and restoring anisotropy torques determined by the energy ε . Therefore in a generic situation the current threshold of merging should be much higher than that of local destabilization. Exceptions to this rule may occur in two cases: first, if the energy landscape ε has special directions where the restoring torque is anomalously small, allowing spin torque to cause large displacement at a current comparable to the critical current of local destabilization; second, if the equilibrium is located close to the critical circle and according to Eq. (10) its local destabilization threshold becomes very high.

The energy landscape of a nanopillar device has a special direction for $\omega_a \ll \omega_p$. In this case the states with \mathbf{n} in the easy plane have almost the same energy and even a small external torque can potentially cause a large equilibrium displacement along the equator of the unit sphere. Consider the “magnetic fan” experiment²² where the polarizer is directed perpendicular to the easy plane, $\mathbf{s} \parallel \hat{z}$ (Fig. 8). In this geometry the spin torque indeed shifts both the minima and the saddle point along the equator until the saddle L merges with M_1 [Fig. 8(a)]. The $g = \text{const}$ approximation is special since the critical circle coincides with the equator. The minimum cannot be destabilized locally since it stays on the critical circle all the time until it merges with a saddle. After the merging event, the system jumps to a precession cycle of large size, called an out-of-plane precession (OPP). In a model with angle-dependent $g(\vartheta)$ the energy minimum points are away from the critical circle. Thus a competing scenario is allowed: Point M_1 can be locally destabilized before it encounters point L . In this case a small precession cycle around M_1 , called an in-plane precession (IPP), will be produced [Fig. 8(b)].¹⁸ Which of the two destabilization events comes first depends on the parameters of the system. Note that this example is special for both reasons discussed in the previous paragraph: There is a special direction, and the equilibrium may be close to the critical circle.

The critical current of local destabilization can be obtained from Eq. (10). For \mathbf{n} on the equator one can estimate

$$\nabla^2 \varepsilon = \omega_p \left(1 + O\left(\frac{\omega_a}{\omega_p}\right) \right),$$

$$\nabla \cdot \mathbf{f}_{st} = -g'(\pi/2),$$

which gives a critical current

$$\omega_{I(IPP)} \approx -\alpha \frac{\omega_p}{g'(\pi/2)}. \quad (15)$$

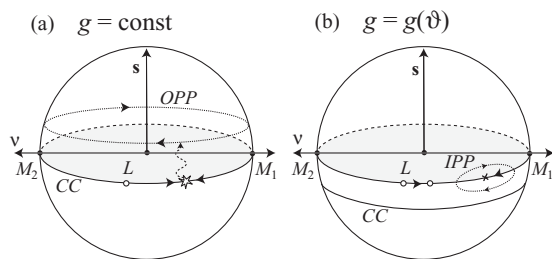


FIG. 8. “Magnetic fan” geometry. (a) At $g = \text{const}$ point M_1 stays on CC until it collides with L , creating a large “OPP cycle” (dotted line). (b) At $g = g(\vartheta)$ M_1 is away from CC . Its local destabilization can create a small “IPP cycle.”

The critical current of merging can be estimated as follows. Both the saddle and the minimum stay on the equator where the spin torque is given by $\boldsymbol{\tau}_{st} = -\omega_I g(\pi/2) \mathbf{e}_\theta$ and the conservative torque equals $\boldsymbol{\tau}_c = \omega_a \cos \phi \sin \phi \mathbf{e}_\theta$. The positions of the M_1 and L points are determined from the torque balance equation

$$\omega_a \cos \phi \sin \phi - \omega_I g(\pi/2) = 0.$$

From this one finds that points M_1 and L merge at

$$\omega_{I(OPP)} = \frac{\omega_a}{2g(\pi/2)}. \quad (16)$$

At the opposite current $\omega_I = -\omega_{I(OPP)}$ the minimum M_1 merges with the another saddle point, L' , located opposite to L .

Equations (15) and (16) show that for

$$\frac{\omega_a}{\omega_p} \sim \alpha \frac{2g(\pi/2)}{g'(\pi/2)}$$

the critical currents of the local and merging destabilization can be of the same order, and the competition between the two destabilization scenarios is possible. Note that the local destabilization can happen only at one sign of the current [assuming $g'(\pi/2) > 0$, the IPP critical current is negative]. The merging destabilization happens at both current directions.

These properties lead to the following prediction. If $\omega_{I(OPP)} < |\omega_{I(IPP)}|$, the system switches to the OPP precession for both current directions. If an opposite inequality holds, a switch to the IPP precession will be observed for one current direction, and a switch to an OPP direction will happen for the opposite current direction. Using Slonczewski’s g and experimental parameters of Ref. 22 we find $\omega_{I(OPP)}/\omega_{I(IPP)} \approx 0.1$, which yields an OPP cycle scenario in accord with experiment. If the easy axis anisotropy ω_a is increased, for example by making the free layer in the shape of an elongated ellipse, a regime of $\omega_{I(OPP)} > |\omega_{I(IPP)}|$ will be reached, and the OPP or IPP cycles will be created depending on the current direction.

Another way of creating a competition between the local destabilization and merging is to tilt the polarizer direction \mathbf{s} away from the \hat{z} axis (Fig. 9). In this case both equilibria are away from the critical circle even in the $g = \text{const}$ approximation. One of them always falls into the local destabilization region and may produce a small-size IPP cycle above the critical current. Similar to the case of the magnetic fan (Fig. 8), both equilibria will be shifted by spin

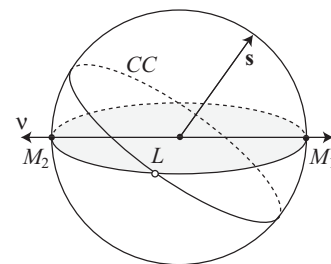


FIG. 9. Tilted polarizer geometry. The minimum points $M_{1,2}$ are away from CC and can be destabilized locally.

torque, and will eventually merge with the saddle points. The competition between the local destabilization and merging destabilization is now controlled by the polarizer tilt angle. This qualitative approach should be very useful for developing a physical understanding of the rich switching diagrams^{23–25} obtained for the tilted polarizer case by conventional methods.

V. CONCLUSIONS

We have discussed two scenarios of stabilization and destabilization of equilibrium magnetization directions by the spin-transfer torque. Equilibrium points can either change their stability locally or experience a collision with the other equilibrium points.

In the case of a local scenario the destabilization of the energy minima and the stabilization of the energy maxima are symmetric processes described by the same *invariant criterion* [Eqs. (8), (9), and (10)]. The ability of current to destabilize the energy minima or stabilize the energy maxima is determined by a single figure of merit, the *switching ability* which is equal to the divergence of the spin torque $\nabla \cdot \tau_{st}$, and can be expressed through the spin-transfer efficiency coefficient $g(\vartheta)$ [Eq. (11)]. Our invariant stability criterion is particularly simple and useful in the limit of small α when the displacements of equilibria caused by spin torque are small. In this case the unit sphere turns out to be divided into the regions of stabilization and destabilization separated by the *critical circles*. A good approximation for the efficiency $g(\vartheta)$ should accurately reproduce the position of the critical circle. For example, the often used approximation $g = \text{const}$ fails not only for exotic “wavy” functions $g(\vartheta)$, but also when it introduces a significant error into the the critical circle location.

In the case of the merging scenario, the displacements of equilibria under the influence of spin torque are normally large and do not depend on the value of α . As a result, it may be easier to detect the destabilization events by following the current-dependent positions of the equilibria, rather than by applying the linear-stability criteria. Merging regularly leads to a destabilization of a minimum, but does not normally stabilize the saddle points. An important exception happens when the polarizer points in the saddle-point direction. In this case an expression (14) for the stabilization current is derived.

The critical currents I_c^{local} in the local scenario are proportional to the small Gilbert damping α and are normally much smaller than the critical currents I_c^{merge} in the merging scenario. In exceptional cases a competition between the two scenarios can take place. This happens either when there is a special direction with small restoring anisotropy torque an I_c^{merge} is lowered, or when the point is close to the critical circle and I_c^{local} is raised. When present, the competition leads to rich switching diagrams.

Overall, our approach allows one to develop a qualitative picture of spin-transfer switching in complicated devices. By considering a range of examples we have shown that the method explains previously known results and makes a number of interesting new predictions.

ACKNOWLEDGMENTS

It is our pleasure to thank S. Garzon, R. A. Webb, A. Slavin, and R. R. Ramazashvili for stimulating discussions. This research was supported by NSF Grant No. DMR-0847159.

APPENDIX A: EIGENVALUES OF A 2×2 MATRIX

For an arbitrary dynamic matrix \hat{D} given by

$$\hat{D} = \begin{vmatrix} a & b \\ c & d \end{vmatrix}$$

the eigenvalues are obtained from the equation

$$(\lambda - a)(\lambda - b) - bc = 0$$

or equivalently

$$\lambda^2 - \lambda \text{Tr} \hat{D} + \det \hat{D} = 0.$$

This gives

$$\lambda_{1,2} = \frac{\text{Tr} \hat{D}}{2} \pm \sqrt{\left(\frac{\text{Tr} \hat{D}}{2}\right)^2 - \det \hat{D}}. \quad (\text{A1})$$

The eigenvalues depend on just two combinations of the matrix elements, $\text{Tr} \hat{D}$ and $\det \hat{D}$. Using the expressions (A1) the domains of different equilibrium types can be found on the parameter plane as shown in Fig. 10. The areas of stable equilibria are shown in gray and occupy the upper left quadrant $\text{Re} \hat{D} < 0$, $\det \hat{D} > 0$.

APPENDIX B: INVARIANT CRITERIA IN THE LIMIT OF SMALL DAMPING

Equation (8) for the critical current reads

$$\text{Tr}[\hat{D}_{\text{cov}}] = -\alpha \nabla^2 \varepsilon|_{n_{\text{eq}}(I)} + \omega_I \nabla \cdot \mathbf{f}_{st}|_{n_{\text{eq}}(I)} = 0.$$

The two terms on the left-hand side come from the conservative and spin-transfer torques. This condition can be also written down in terms of the original dynamic matrix as $\text{Tr}[\hat{D}] = 0$. Since the trace operation is linear, a separation into the contributions from the conservative and spin-transfer torques

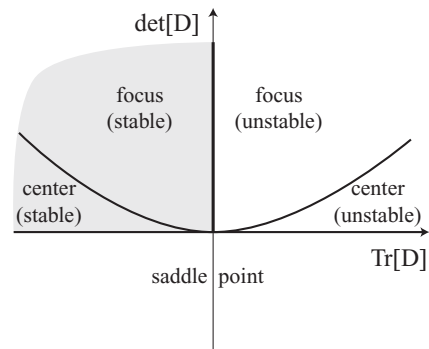


FIG. 10. Equilibrium stability diagram on a plane of trace and determinant of the dynamic matrix. Domain of stability shown in gray consists of stable center domain (real eigenvalues $\lambda_{1,2} < 0$) and stable focus domain (complex conjugated eigenvalues with $\text{Re} \lambda < 0$). Domain of equilibrium instability consists of unstable center domain (real eigenvalues $\lambda_{1,2} > 0$), unstable focus domain (complex conjugated eigenvalues with $\text{Re} \lambda > 0$), and the domain of saddle points (real eigenvalues with opposite signs).

is also possible:

$$\text{Tr}[\hat{D}] = \text{Tr}[\hat{D}_c] + \text{Tr}[\hat{D}_{st}].$$

Here matrix D_c comes from the $\boldsymbol{\tau}_c + \alpha[\mathbf{n} \times \boldsymbol{\tau}_c]$ part of \mathbf{F} , and D_{st} comes from the $\boldsymbol{\tau}_{st} + \alpha[\mathbf{n} \times \boldsymbol{\tau}_{st}]$ part. We will explicitly show the proportionality of D_{st} to the current by writing $\hat{D}_{st} = \omega_I \hat{d}_{st}$.

At small current values the equilibrium displacement $d\mathbf{n} = \mathbf{n}_{eq}(I) - \mathbf{n}_{eq}(0)$ is small, $d\mathbf{n} \sim \omega_I$, and one can expand near $\mathbf{n}_{eq}(0)$. Expansions of the conditions using \hat{D}_{cov} and \hat{D} up to the first order in ω_I give respectively

$$-\alpha \nabla^2 \varepsilon|_0 - \alpha \left. \frac{\partial \nabla^2 \varepsilon}{\partial \mathbf{n}} \right|_0 d\mathbf{n} + \omega_I \nabla \cdot \mathbf{f}_{st}|_0 = 0$$

and

$$\text{Tr}[\hat{D}_c]|_0 + \left. \frac{\partial \text{Tr}[\hat{D}_c]}{\partial \mathbf{n}} \right|_0 d\mathbf{n} + \omega_I \text{Tr}[\hat{d}_{st}]|_0 = 0,$$

where subscript “0” means the expression was evaluated at $\mathbf{n}_{eq}(0)$.

The first terms in both conditions represent the values of $\text{Tr}[\hat{D}_{cov}]$ and $\text{Tr}[\hat{D}]$ at zero current equilibrium. Since \hat{D}_{cov} and \hat{D} coincide at an equilibrium point, these terms are equal to each other. In contrast, the second terms are substantially different: In the upper condition the second term is proportional to the product $\alpha \omega_I$, while in the lower condition the second term is proportional to ω_I alone. This is why for small α the second term can be dropped from the upper condition, but has to be kept in the lower one. The third terms are both proportional to ω_I but $\nabla \cdot \mathbf{f}_{st}|_0$ and $\text{Tr}[\hat{d}_{st}]|_0$ are not necessarily equal to each other. Overall, the first condition with neglected second term, i.e., Eq. (9),

$$-\alpha \nabla^2 \varepsilon|_0 + \omega_I \nabla \cdot \mathbf{f}_{st}|_0 = 0,$$

and the second condition with all three terms give the critical current value with the same accuracy.

*yar@physics.sc.edu

¹L. Berger, *J. Appl. Phys.* **49**, 2156 (1978); *Phys. Rev. B* **33**, 1572 (1986); **54**, 9353 (1996).

²J. C. Slonczewski, *J. Magn. Magn. Mater.* **159**, L1 (1996).

³J. D. Crawford, *Rev. Mod. Phys.* **63**, 991 (1991).

⁴D. C. Ralph and M. D. Stiles, *J. Magn. Magn. Mater.* **320**, 1190 (2008).

⁵The “fieldlike” torque, not included here, changes the energy as $\varepsilon \rightarrow \varepsilon + I \Delta \varepsilon$ and will not alter our first-order result (9) when $\Delta \mathbf{n}$ is small.

⁶Ya. B. Bazaliy, B. A. Jones, and S. C. Zhang, *Phys. Rev. B* **69**, 094421 (2004).

⁷G. Bertotti, C. Serpico, I. D. Mayergoyz, A. Magni, M. d’Aquino, and R. Bonin, *Phys. Rev. Lett.* **94**, 127206 (2005).

⁸C. Serpico, *J. Magn. Magn. Mater.* **290**, 48 (2005).

⁹R. Bonin, C. Serpico, G. Bertotti, I. D. Mayergoyz, and M. d’Aquino, *Eur. Phys. J. B* **59**, 435 (2007).

¹⁰J. A. Katine, F. J. Albert, R. A. Buhrman, E. B. Myers, and D. C. Ralph, *Phys. Rev. Lett.* **84**, 3149 (2000).

¹¹N. Smith, J. A. Katine, J. R. Childress, and M. J. Carey, *IEEE Trans. Magn.* **41**, 2935 (2005); **42**, 114 (2006).

¹²I. Sodemann and Ya. B. Bazaliy, *J. Appl. Phys.* **105**, 07D114 (2009).

¹³Ya. B. Bazaliy, B. A. Jones, and Shou-Cheng Zhang, *J. Appl. Phys.* **89**, 6793 (2001).

¹⁴T. Devolder, A. Meftah, K. Ito, J. A. Katine, P. Crozat, and C. Chappert, *J. Appl. Phys.* **101**, 063916 (2007).

¹⁵O. Boulle, V. Cros, J. Grollier, L. G. Pereira, C. Deranlot, F. Petroff, G. Faini, J. Barnaś, and A. Fert, *Nature Phys.* **3**, 492 (2007).

¹⁶J. Manschot, A. Brataas, and G. E. W. Bauer, *Appl. Phys. Lett.* **85**, 3250 (2004); *Phys. Rev. B* **69**, 092407 (2004).

¹⁷M. Gmitra and J. Barnaś, *Phys. Rev. Lett.* **96**, 207205 (2006).

¹⁸We confirmed these qualitative predictions numerically.

¹⁹X. Wang, G. E. W. Bauer, and T. Ono, *Jpn. J. Appl. Phys.* **45**, 3863 (2006).

²⁰H. Morise and S. Nakamura, *Phys. Rev. B* **71**, 014439 (2005).

²¹N. D. Mermin, *Rev. Mod. Phys.* **51**, 591 (1979).

²²D. Houssameddine, U. Ebels, B. Delaët, B. Rodmacq, I. Firastrau, F. Ponthenier, M. Brunet, C. Thirion, J.-P. Michel, L. Prejbeanu-Buda, M.-C. Cyrille, O. Redon, and B. Dieny, *Nature Mater.* **6**, 447 (2007).

²³Y. B. Bazaliy and B. A. Jones, *Physica B* **329-333**, 1290 (2003).

²⁴Y. Zhou, S. Bonetti, C. L. Zha, and J. Åkerman, *New J. Phys.* **11**, 103028 (2009).

²⁵P.-B. He, R.-X. Wang, Z.-D. Li, Q.-H. Liu, A.-L. Pan, Y.-G. Wang, and B.-S. Zou, *Eur. Phys. J. B* **73**, 417 (2010).